ELSEVIER

Journal of Organometallic Chemistry 559 (1998) 165–171

Journal of Organo metallic Chemistry

# Synthesis, structural characterization and semiempirical calculations of the ruthenium azide complex $[Ru(tpy)(PPh_3)_2(N_3)][ClO_4]$

Won K. Seok [a], Sun Bin Yim [a], Thomas M. Klapötke [b,*], Peter S. White [c]

[a] *Department of Chemistry, Dongguk University, 26 Pil-Dong, Chung-Ku, Seoul 100-715, South Korea*
[b] *Institute of Inorganic Chemistry, University of Munich (LMU), Meiserstraße 1, D-80333 Munich, Germany*
[c] *Department of Chemistry, University of North Carolina, Chapel Hill, NC 27599-3290, USA*

Received 27 November 1997

---

**Abstract**

The reaction of $[Ru(tpy)(PPh_3)_2Cl][PF_6]$ (tpy, 2,2′:6′,2″-terpyridine) with $NaN_3/NaClO_4$ in acetone/water produced the ruthenium(II) complex $[Ru(tpy)(PPh_3)_2(N_3)][ClO_4]$ (**1**), which contains a coordinated azide unit with $Ru{-}N = 2.132(5)$ Å. The new Ru azide complex **1** was identified and characterized by elemental analysis, IR, Raman and multinuclear NMR ($^1H$, $^{14}N$, $^{31}P$) data. Crystals were grown from an acetonitrile/diethyl ether solution and the crystal structure was determined by a low-temperature single crystal X-ray diffraction study. Crystallographic data for **1**: triclinic, $P\bar{1}$, $a = 10.9905(5)$, $b = 13.4741(6)$, $c = 17.8532(9)$ Å, $\alpha = 90.6760(10)$, $\beta = 96.4000(10)$, $\gamma = 105.5270(10)°$, $V = 2529.07(21)$ Å$^3$, $\rho = 1.422$ g cm$^{-3}$, $Z = 2$. The experimentally obtained structural parameters for compound **1** compare reasonably well with those calculated at the semi-empirical ZINDO/1 level of theory. © 1998 Elsevier Science S.A. All rights reserved.

*Keywords:* Azides; Raman Spectra; Ruthenium; ZINDO Calculations

---

## 1. Introduction

Cationic ruthenium complexes with tridentate (*N,N′,N″*) and also with bidentate (*N,N′*) 2,2′:6′,2″-terpyridine (tpy) ligand systems have been known for several years. For example, $[Ru(NO_2)(PMe_3)_2(tpy)][ClO_4]$ ([1]a) and $[Ru(N,N',N''\text{-tpy})(N,N'\text{-tpy})Cl][PF_6]$ ([1]b) have been reported recently. Cationic azidoruthenium(III) complexes with additional $NH_3$ have already been reported as early as in 1970 ([1]c).

After early work in transition metal azide chemistry where the characterization was largely based on $^{14}N$-NMR data {see for example $[Pd(PPh_3)_2(N_3)_2]$ and *cis*-$[Pt(PBu_3)_2(N_3)_2]$ ([2]a)}, recently interest has emerged in the preparation and structural characterization of inorganic and organometallic transition metal azide complexes. For example, *trans*-$[Ru(depe)_2(N_3)_2]$ (depe, 1,2-bis(diethylphosphino)ethane) ([2]b) and the closely related complex $[Fe(dmpe)(N_3)_2]$ (dmpe, 1,2-bis(dimethylphosphino)ethane) [3], as well as the Cp derivative $[Ru(C_5H_5)_2(N_3)]$, have been prepared and structurally characterized [4]. Very recently, four new inorganic titanium azide complexes, $[Ti(NMe_2)_2(N_3)_2]_n$, $[Ti(NMe_2)_2(N_3)_2(py)_2]_n$, $[Ti(NMe_2)_2(N_3)_2(bipy)]_n$ and $[Ti(NMe_2)_3(N_3)(bipy)]_n$ were reported ([5]a). Moreover, quite recently also diazido complexes of manganese were synthesized ([5]b,c).

In this contribution we wish to report the synthesis, spectroscopic and structural characterization as well as results from semi-empirical calculations of the new ruthenium(II) azide complex $[Ru(tpy)(PPh_3)_2(N_3)][ClO_4]$ (**1**).

---

* Corresponding author. Fax: +49 89 5902382.

*PII* S0022-328X(98)00408-2

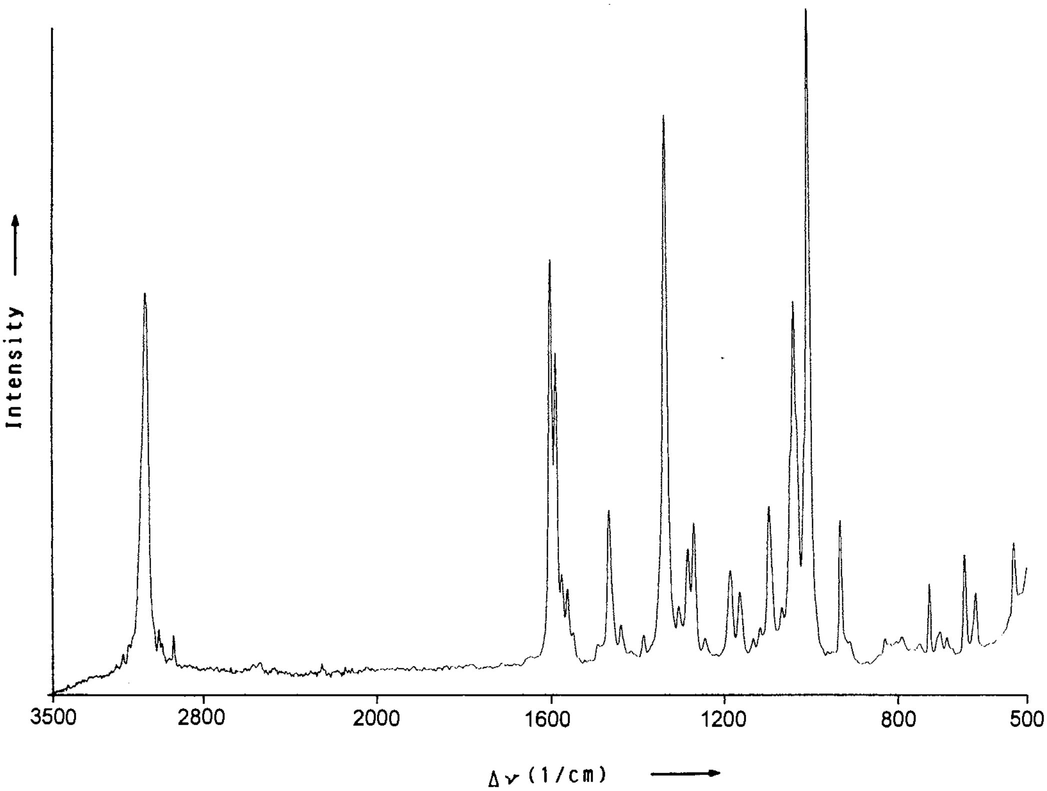

Fig. 1. Raman spectrum of $[Ru(tpy)(PPh_3)_2(N_3)][ClO_4]$ (**1**) (for details see Section 3)

## 2. Results and discussion

The ruthenium(II) complex $[Ru(tpy)(PPh_3)_2(N_3)][ClO_4]$ (**1**) was prepared from the chloro hexafluorophosphate precursor ([6]a) in a convenient two-step one-pot reaction according to Eqs. (1a) and (1b) (cf. also the chemistry and preparation of the isovalent electronic $[Re(tpy)(PPh_3)_2(Cl)])$ [6b].

$$[Ru(tpy)(PPh_3)_2Cl][PF_6] + NaN_3 \xrightarrow{\text{acetone/water}} [Ru(tpy)(PPh_3)_2(N_3)][PF_6] + NaCl \quad (1a)$$

$$[Ru(tpy)(PPh_3)_2(N_3)][PF_6] + NaClO_4 \text{ (saturated solution in } H_2O) \xrightarrow{\text{acetone/water}} [Ru(tpy)(PPh_3)_2(N_3)][ClO_4]\downarrow + NaPF_6 \quad (1b)$$

### *2.1. Spectroscopy*

The new ruthenium azide complex **1** was identified and characterized by elemental analysis, IR, Raman and multinuclear NMR ($^1$H, $^{14}$N, $^{31}$P) data (see Section 3). As the most intense and characteristic absorptions the IR spectrum shows the asymmetric azide stretching mode at 2042 $cm^{-1}$.

The Raman spectrum of **1** (Fig. 1) shows the very characteristic symmetric azide stretching mode as an intense peak at 1335 $cm^{-1}$ and also a very strong peak at 3064 $cm^{-1}$ for the aromatic C–H stretching modes. In addition there are well resolved signals for the C–C stretches of the aromatic phenyl rings and the tpy ligand system (1466–1600 $cm^{-1}$). The totally symmetric $\nu_1$ stretching mode of the $ClO_4^-$ anion appears as the strongest Raman peak of this tetrahedral system at 932 $cm^{-1}$ [7].

The $^1$H-NMR spectrum showed a complex multiplet in the area between 6.9 and 8.1 ppm for the aromatic protons of the phenyl rings and the tpy ligand system. This multiplet appeared nearly unchanged compared to the precursor complex $[Ru(tpy)(PPh_3)_2Cl][PF_6]$. However, the low-field pseudo-doublet of the 2 or 6″ protons significantly changed from 9.02 and 9.03 ppm in $[Ru(tpy)(PPh_3)_2Cl][PF_6]$ to 8.72 and 8.75 ppm in $[Ru(tpy)(PPh_3)_2(N_3)][ClO_4]$.

Complex **1** was also characterized by $^{14}$N-NMR spectroscopy (Table 1). For the covalently bound azide species three well resolved resonances have been found in the $^{14}$N-NMR spectrum and assignment of the individual resonances to Na, Nb and Nc (connectivity: Ru–Na–Nb–Nc) was made on the basis of the arguments given in earlier work by Witanowski [8] and other reports on $^{14}$N data of covalent azides [9–13]. The individual chemical shifts as well as line-widths found for $[Ru(tpy)(PPh_3)_2(N_3)][ClO_4]$ nicely compare to related covalently bound metal–azide complexes (Table 1) ([2]a, [12,14]). Presumably as a result of the large

Table 1
$^{14}$N-NMR spectroscopic data of $[Ru(tpy)(PPh_3)_2(N_3)][ClO_4]$ (**1**) and related compounds chemical shifts $\delta$ in ppm relative to $MeNO_2$ (connectivity: X–Na–Nb–Nc)

| | Na | Nb | Nc | Ref. |
|---|---|---|---|---|
| $[Ru(tpy)(PPh_3)_2(N_3)][ClO_4]$ (**1**) | −337 (300)[a] | −136 (20) | −224 (60) | This work |
| $(CF_3)_3GeN_3$ | −332.8 (350) | −145.1 (28) | −186.8 (54) | [12] |
| $As(N_3)_3$ | −318.0 (150) | −131.1 (15) | −165.2 (30) | [11] |
| $[Pd(PPh_3)_2(N_3)_2]$ | −363 (145) | −140 (110) | −230 (75) | [14] |
| *cis*-$[Pt(PBu_3)_2(N_3)_2]$ | −326 (220) | −135 (145) | −226 (110) | [14] |

[a] Line-widths $\Delta\nu$ in Hz (in perentheses).

quadrupole moment of $^{14}$N, spin–spin splitting which has been estimated to be $<30$ Hz was not observed (cf. line-widths, Table 1) [15]. The three N atoms of the tpy ligand system, however, could not be observed. In this context it should be noted that the relative line-widths in the $^{14}$N-NMR spectra are related to the local symmetry around the nitrogen atom, with highly symmetric N atoms (i.e. Nb, central N of $N_3$) having sharper lines, whilst the more asymmetric nitrogen atoms (i.e. Nc, terminal N of $N_3$) have broader lines and the very asymmetric N atoms (i.e. Na, bound to Ru and tpy N atoms) have very broad lines [16].

The $^{31}$P-NMR spectrum of **1** showed a singlet resonance at 26.5 ppm for the coordinated $PPh_3$ groups (cf. the free $PPh_3$ ligand shows resonance at −4 ppm). Therefore, the $^{31}$P resonance of **1** appears at slightly lower field than that of the starting material $[Ru(tpy)(PPh_3)_2Cl][PF_6]$ (22.4 ppm).

### 2.2. X-ray structure

The structure of the ruthenium azide complex, $[Ru(tpy)(PPh_3)_2(N_3)][ClO_4]$ (**1**), was determined experimentally by X-ray diffraction analysis at low temperature using a Siemens SMART area detector system. Fig. 2 shows a formula unit of the ruthenium azide cation and Fig. 3(a,b) show the packing diagrams of the ruthenium azide complex, $[Ru(tpy)(PPh_3)_2(N_3)][ClO_4]$. Table 2 summarizes the most important experimentally obtained structural parameters for complex **1**.

As expected for a covalently bound azide (i.e. a coordinated and not an ionic $N_3$ unit), the $[Ru(tpy)(PPh_3)_2(N_3)]^+$ cation displays a bent *trans* configuration with an N–N–N bond angle of 177.8°. The two N–N distances are identical within the standard deviation (1.16 Å). This can be explained by only a weak coordinative bond between N1 and Ru1 which is also in agreement with the only slight bending of the azide group (cf. typical covalent azides show NNN angles of 172 ± 2°) [17,18].

The structural parameters compare also well with those of some related and recently characterized ruthenium and iron azide complexes. For example, in *trans*-$[Ru(depe)_2(N_3)_2]$ (depe, 1,2-bis(diethylphosphino) ethane) the Ru1–N1 bond length is 2.354(1) Å and the N–N distances are N1–N2 = 1.180(5) Å and N2–N3 = 1.170(5) Å, respectively ([2]b). The closely related complex $[Fe(dmpe)(N_3)_2]$ (dmpe, 1,2-bis(dimethylphosphino)ethane) displays a Fe1–N1 bond length of 2.024(3) Å and a N1–N2 bond length of 1.162(5) Å [3]. The molecule $[Ru(C_5H_5)_2(N_3)]$ again has a similar Ru1–N1 bond length of 2.135(3) Å [4]. The azide group is slightly bent (175.2(3)°) and there is a small difference between the N–N distances [1.186(3) and 1.164(3) Å], the longer being adjacent to the Ru atom [4].

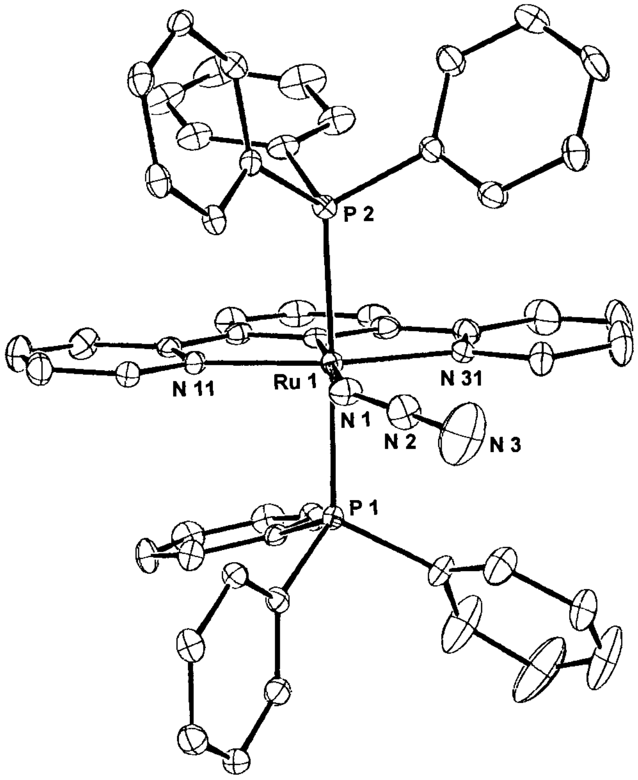

Fig. 2. Structure of a formula unit of a $[Ru(tpy)(PPh_3)_2(N_3)]^+$ cation in the crystal (ORTEP representation) [19].

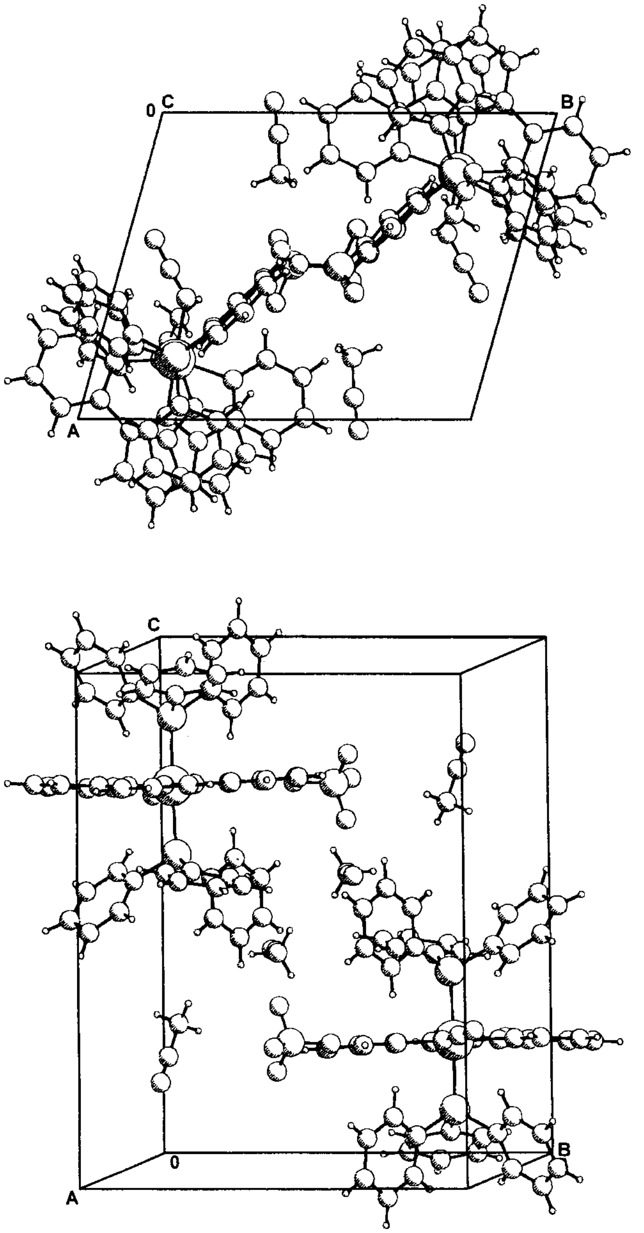

Fig. 3. Top: 2-D packing diagram of $[Ru(tpy)(PPh_3)_2(N_3)][ClO_4]$ (PLUTO representation) [20]. Bottom: 3-D packing diagram of $[Ru(tpy)(PPh_3)_2(N_3)][ClO_4]$ (PLUTO representation) [20].

### 2.3. Semi-empirical calculations

The structure of the ruthenium azide complex **1** (*trans* isomer) as well as the structure of the corresponding *cis* isomer and their total energies were calculated at the semi-empirical ZINDO/1 level of theory.

For both calculated ruthenium complexes the triphenyl phosphine ligand was modeled by the electronically very similar and closely related $PMe_3$ (Me = $CH_3$) ligand in order to reduce the number of parameters and to save cpu time.

As expected the *cis* and the *trans* isomers of **1** are very close in their total energy with the *trans* form being thermodynamically slightly favored over the *cis* isomer ($\Delta E(cis\text{–}trans) = 5$ kcal mol$^{-1}$; Table 3). It has to be stressed, however, that the calculations were performed for isolated ions in the gas phase and that the stability might be reversed in the condensed phase due to cation–anion interactions, molecule/ion–solvent interactions or crystal packing effects [21].

For both isomers of **1** (*cis* and *trans*) the stationary points were characterized as true minima (within the ZINDO/1 model) by frequency analyses (in all cases NIMAG = 0; NIMAG, number of imaginary frequencies) [22]. The asymmetric $N_3$ stretching mode which is very strong in the IR spectra was also calculated (Table 3).

To assign the experimentally observed IR frequencies of the complex cation *trans*-$[Ru(tpy)(PPh_3)_2(N_3)]^+$ in the compound $[Ru(tpy)(PPh_3)_2(N_3)][ClO_4]$ the structure of the cation *trans*-$[Ru(tpy)(PPh_3)_2(N_3)]^+$ was optimized in $C_1$ symmetry and the vibrational frequencies and their intensities were calculated at the semi-empirical ZINDO/1 level of theory using a VSTO-3G* basis set. Molecular frequencies depend on the second derivative of the energy with respect to the nuclear positions. Due to the harmonic potential applied (and due to the neglect of electron correlation) raw frequencies computed at the HF and ZINDO levels contain systematic errors. Therefore, it is usual to scale calculated frequencies by empirical factors (*F*) smaller than unity. Use of such factors has been demonstrated to produce good agreement with experiment for a wide range of systems [22,27,28].

Table 2
Selected measured (X-ray) bond lengths (Å) and angles (°) of $[Ru(tpy)(PPh_3)_2(N_3)][ClO_4]$ (**1**)[a]

| Atoms | Bond length (Å) | Atoms | Bond angle (°) |
|---|---|---|---|
| Ru1–P1 | 2.4013(14) | P1–Ru1–P2 | 176.52(5) |
| Ru1–P2 | 2.3972(14) | P1–Ru1–N1 | 89.69(12) |
| Ru1–N11 | 2.102(4) | P1–Ru1–N11 | 89.51(11) |
| Ru1–N21 | 1.965(4) | P1–Ru1–N21 | 90.97(12) |
| Ru1–N31 | 2.087(4) | P1–Ru1–N31 | 91.57(11) |
| Ru1–N1 | 2.132(5) | P2–Ru1–N1 | 87.90(12) |
| N1–N2 | 1.157(7) | P2–Ru1–N11 | 88.41(11) |
| N2–N3 | 1.159(8) | P2–Ru1–N21 | 91.36(12) |
| | | P2–Ru1–N31 | 91.40(11) |
| | | N1–Ru1–N11 | 99.03(17) |
| | | N1–Ru1–N21 | 177.83(18) |
| | | N1–Ru1–N31 | 102.77(18) |
| | | N11–Ru1–N21 | 78.92(17) |
| | | N11–Ru1–N31 | 158.18 |
| | | N21–Ru1–N31 | 79.28(18) |
| | | Ru1–N1–N2 | 139.6(4) |
| | | N1–N2–N3 | 177.8(6) |

[a] Atomic labeling analogous to Fig. 1.

Table 3
Semi-empirically calculated structural parameters and total energies for the *cis* and *trans* isomers of complex **1** (ZINDO/1/VSTO-3G* level of theory)

| Complex | $E$ (kcal mol$^{-1}$) | NIMAG | $\nu$(N$_3$, asym) [cm$^{-1}$] (Int.)[a] | Ru–N1 (Å) | N1–N2 (Å) | N2–N3 (Å) | N1–N2–N3 (°) |
|---|---|---|---|---|---|---|---|
| **1** (*trans*) | | | | | | | |
| ZINDO/ 1 | −17473 | 0 | 2034 | 1.97 | 1.24 | 1.19 | 175.2 |
| Experimental | | | 2053 | 2.13 | 1.16 | 1.16 | 177.8 |
| **1** (*cis*) | | | | | | | |
| ZINDO/ 1 | −17468 | 0 | 2084 | 1.92 | 1.24 | 1.18 | 173.2 |

[a] Scaled with an empirical factor of 0.62.

In the present study a factor of $F(\nu)=0.60$ for the stretching modes and $F(\delta)=0.80$ for in plane ($\delta$) and out of plane ($\gamma$) deformation modes was applied. The results are summarized in Table 4.

## 3. Experimental

All reactions were carried out using standard Schlenk techniques.

### 3.1. Preparation of [Ru(tpy)(PPh$_3$)$_2$(N$_3$)][ClO$_4$] (1)

A sample of [Ru(tpy)(PPh$_3$)$_2$Cl][PF$_6$] (100 mg, 0.10 mmol) [6] was dissolved in acetone (ca. 15 cm$^3$) and subsequently sodium azide (18.8 mg, 0.29 mmol) in water (ca. 1 cm$^3$) was added. The reaction mixture was refluxed for 1 h and was then allowed to cool to room temperature yielding a purple solution. At this stage the precipitation of any solid must be avoided. Subsequently, a saturated solution of sodium perchlorate in water (excess) was added at 0°C and the reaction mixture was stirred for five minutes. At this time the solution turned darker and the color slowly changed from purple to dark-brown. The reaction product which was insoluble in the acetone/water mixture was filtered off and carefully washed with small amounts of acetone and ether and then dried in vacuo. Recrystallization of the crude material from dry acetonitrile/ ether (ca. 10 cm$^3$) yielded dark brown crystals of complex **1** (84 mg, 84%).

Elemental analysis (Carlo Erba, EA 1180), RuP$_2$C$_{55}$H$_{47}$ClN$_8$O$_4$, (1082.49) Anal. Calc.: C 60.5, H 4.2 , N 9.4. Found: C 61.0, H 4.4, N 10.3%.

IR (Hartmann and Braun, KBr, cm$^{-1}$): 3058 m, 2042 vs, 1604 w, 1561 m, 1481 m, 1434 s, 1386 m, 1281 w, 1089 s, 771 m, 747 s, 698 s, 624 m, 517 s, 493 m.

Raman (1064 nm, 200 mW, 20°C, 5000 scans, cm$^{-1}$, (Int.)): 3064 (6), 1600 (6), 1588 (5), 1466 (3), 1335 (8), 1270 (5), 1186 (4), 1096 (5), 1038 (6), 1004 (10), 932 (3), 726 (2), 644 (2). A Raman spectrum was also recorded at −150°C which showed virtually an identical spectrum.

The $^1$H-NMR spectra were recorded in 5 mm NMR tubes in DMSO-d$_6$ solution (saturated solution) at 25°C using a Varian Gemini 200 MHz spectrometer. $^1$H-NMR (ppm): 6.9–8.8 m; 8.72 and 8.75 ‘d’.

#### 3.1.1. $^{14}$N-NMR spectroscopy

The $^{14}$N-NMR spectrum was recorded in a 10 mm NMR tube in CD$_2$Cl$_2$ solution (saturated solution) at −20°C using a Bruker SY 200 spectrometer operating at 14.462 MHz. A good spectrum could be obtained with a pulse width of 45 μs after 90000 scans and is reported ppm in the $\delta$ scale referred to external MeNO$_2$ in CD$_2$Cl$_2$ solution. Peak positions appearing downfield (high-frequency) of the reference are reported as plus and those upfield (low-frequency) of the reference are reported as minus. A routine baseline correction was applied. $^{14}$N-NMR [ppm, $\Delta\nu_{1/2}$ (Hz)]: −136 (20), −224 (60), −337 (300).

The $^{31}$P-NMR spectra were recorded in 5 mm NMR tubes in DMSO-d$_6$ solution (saturated solution) at 25°C using a Varian Gemini 300 MHz spectrometer operating at 121.44 MHz and are referred to H$_3$PO$_4$ (85% solution in water). $^{31}$P-NMR (ppm): 26.53 s.

### 3.2. Crystallography

#### 3.2.1. X-ray structural determination of [Ru(tpy)(PPh$_3$)$_2$(N$_3$)][ClO$_4$]·2CH$_3$CN (1)

Crystal data for the ruthenium azide complex, [Ru(tpy)(PPh$_3$)$_2$(N$_3$)][ClO$_4$]·2CH$_3$CN: Molecular formula RuP$_2$C$_{55}$H$_{47}$ClN$_8$O$_4$, $M=1082.49$, triclinic, $a=10.9905(5)$, $b=13.4741(6)$, $c=17.8532(9)$ Å, and $\alpha=90.6760(10)$, $\beta=96.4000(10)$, $\gamma=105.5270(10)$°; $V=2529.07(21)$ Å$^3$, space group P$\bar{1}$, $Z=2$, $D_{calc.}=1.422$ g cm$^{-1}$. Crystal dimensions 0.20×0.15×0.10 mm. $\mu$(Mo–K$_\alpha$) = 0.48 mm$^{-1}$, $\lambda=0.71073$ Å, $F(000)=1110.75$.

Data collection and processing: Siemens SMART diffractometer, −100°C (173 K), $\omega$ scan mode, $2\theta_{max.}=50.0$°, graphite monochromated Mo–K$_\alpha$ radiation, 18108 independent measured reflections, 8738 unique reflections, 6236 reflections with $[I>3.0\sigma(I)]$. Absorption corrections were made using SADABS.

Table 4
Calculated (ZINDO/1/VSTO-3G*) and experimentally observed IR frequencies of the cation $[Ru(tpy)(PPh_3)_2(N_3)]^+$

| Experimental IR ($cm^{-1}$) | Calc. IR ($cm^{-1}$) | Calc. $R_{int}^{a}$ | Scaled IR ($cm^{-1}$)$^{b}$ | Assignment |
|---|---|---|---|---|
| 3058 m | 4814 | 42 | 2985 | $\nu$(CH, Ph+tpy) |
| 2042 vs | 3313 | 956 | 2054 | $\nu_{as}$ (NNN) |
| 1604 w | | | | |
| 1561 m | 2540 | 33 | 1575 | $\nu_{sym}$(CN, tpy) |
| 1481 m | 2524 | 31 | 1565 | $\nu_{sym}$(CC+CN, tpy)+some $\nu$(CC, Ph) |
| 1434 s | 2517 | 30 | 1560 | $\nu_{sym}$(CC+CN, tpy)+some $\nu$(CC, Ph) |
| 1386 m | 2503 | 41 | 1552 | $\nu$(CNC, tpy); $\nu$(CC, Ph) |
| 1281 w, br | 2106 | 48 | 1306 | $\nu_{sym}$(NNN) |
| | 2102 | 38 | 1303 | $\nu_{as}$(CC+CN, tpy) |
| | 2101 | 23 | 1302 | $\nu_{as}$(CC+CN, tpy) |
| 1089 s$^{c}$ | 1163 | 35 | 930 (F = 0.8) | $\nu$(PC); $\delta$(PRuP); $\gamma$(Ph); $\nu$(CC, Ph) |
| 771 m | 973 | 21 | 779 | $\gamma$(tpy) |
| 747 s | 939 | 31 | 751 | $\delta$(CPC) |
| 698 s | 856 | 21 | 685 | $\gamma$(Ph) |
| 624 m$^{c}$ | | | | $ClO_4^-$ |
| 517 s | 835 | 32 | 518 (F = 0.62) | $\nu$(RuN); $\delta$(NNN) |
| 493 m | 822 | 23 | 510 | $\nu$(RuN); $\delta$(NNN); $\delta$(CC, Ph+tpy) |
| 585 | 26 | 468 | $\delta$(NNN) | |

[a] Only calc. $R_{int} > 20$ are listed.

[b] $F(\nu) = 0.60$ for the stretching modes and $F(\delta) = 0.80$ for in plane ($\delta$) and out of plane ($\gamma$) deformation modes.

[c] Absorptions (partly) due to the $ClO_4^-$ anion, $\nu_1 = 928$ (IR−, Ra+), $\nu_2 = 459$ (IR−, Ra+), $\nu_3 = 1119$ (IR+, Ra+), $\nu_4 = 625$ (IR+, Ra+) [29].

Structure analysis and refinement: The structure was solved by direct methods, and all non-H atoms refined anisotropically. Refinement was by least-squares with 118 atoms, 640 parameters and 6142 out of 8738 reflections to $R_F = 0.053$, $(R_F = \Sigma[F_o - F_c]/\Sigma[F_o])$, $wR = 0.056$, $(wR = [\Sigma\{w[F_o - F_c]^2\}/\Sigma\{wF_o^2\}]^{1/2})$; for all reflections: $R_F = 0.091$, $wR = 0.068$. In the last D-map, the deepest hole was $-0.58$ e Å$^{-3}$, and the highest peak was 0.95 e Å$^{-3}$. Computations were carried out using the NRCVAX program system and published scattering factors [23,24].

Further details of the crystal structure determinations are available upon request from the Fachinformationszentrum Karlsruhe, Gesellschaft für wissenschaftlich-technische Information mbH, D-76344 Eggenstein-Leopoldshafen, Germany, on quoting the journal, the title, the authors and the depository numbers CSD-407523.

### 3.3. Semi-empirical calculations

All semi-empirical calculations were performed with the program package HyperChem (version 4.0 and 5.0) ([25]a,b). The semi-empirical calculations were performed at the ZINDO/1 level of theory using a VSTO-3G* basis set [26]. The ZINDO/1 is a variation of INDO extended to transition metals. Equivalent to the most recent version of the INDO/1 method which differs from the original by using constant orbital exponents. The model is characterized by inclusion of all the one-center exchange terms as well as an accurate description of integrals involving 3d atomic orbitals. The model is within the unrestricted Hartree–Fock formalism.

## Acknowledgements

The authors thank Dr A. Schulz and W. Wünschheim for the installation of the quantumchemical programs. This work was financially supported by the Dongguk University, the University of Munich and the North Atlantic Treaty Organization (NATO, CRG 920034-3 to T.M. Klapötke and P.S. White).

## References

[1] (a) R.A. Leising, S.A. Kubow, M.R. Churchill, L.A. Buttrey, J.W. Ziller, K.J. Takeuchi, Inorg. Chem. 29 (1990) 1306. (b) E.C. Constable, A.M.W. Cargill Thompson, Inorg. Chim. Acta 223 (1994) 177. (c) L.A.P. Kane-Maguire, P.S. Sheridan, F. Basolo, R.G. Pearson, J. Am. Chem. Soc. 92 (1970) 5865.

[2] (a) W. Beck, W. Becker, K.F. Chew, W. Derbyshire, N. Logan, D.M. Revitt, D.B. Sowerby, J. Chem. Soc. Dalton Trans. (1972) 245. (b) I.E. Buys, L.D. Field, A.V. George, T.W. Hambley, G.R. Purches, Aust. J. Chem. 48 (1995) 27.

[3] I.E. Buys, L.D. Field, A.V. George, T.W. Hambley, S.R. Pike, unpublished data (cf. ref [2]b).

[4] M.M.T. Khan, M.M. Bhadbhade, M.R.M. Siddiquit, K. Venkatasubramanian, J.A. Tikhonova, Acta Crystallogr. Sect. C 50 (1994) 502.

[5] (a) C.J. Carmalt, A.H. Cowley, R.D. Culp, et al., J. Chem. Soc. Dalton Trans. (1997) 3108. (b) B. Cortes, J.L. Pizarro, L. Lezama, M.I. Arriortua, T. Rojo, Inorg. Chem. 33 (1994) 2697. (c) R. Cortes, M. Drillon, X. Solans, L. Lezama, T. Rojo, Inorg. Chem. 36 (1997) 677.

[6] (a) B.P. Sullivan, J.M. Calvert, T.J. Meyer, Inorg. Chem. 19 (1980) 1404. (b) L.E. Helberg, J. Barrera, M. Sabat, W.D. Harman, Inorg. Chem. 34 (1994) 2033.

[7] H. Siebert, Z. Anorg. Allg. Chem. 275 (1954) 225.

[8] M. Witanowski, J. Am. Chem. Soc. 90 (1968) 5683.

[9] H. Holfter, T.M. Klapötke, A. Schulz, Polyhedron 15 (1996) 1405.

[10] P. Geissler, T.M. Klapötke, H.-J. Kroth, Spectrochim. Acta Part A 51 (1995) 1075.

[11] T.M. Klapötke, P. Geissler, J. Chem. Soc. Dalton Trans. (1995) 3365.

[12] T.M. Klapötke, A. Schulz, Inorg. Chem. 35 (1996) 4995.

[13] T.M. Klapötke, A. Schulz, J. McNamara, J. Chem. Soc. Dalton Trans. (1996) 2985.

[14] N. Logan, in: M. Witanowski, G.A. Webb (Eds.), Nitrogen NMR, Plenum Press, London, 1973, pp. 320–366.

[15] D. Herbison-Evans, R.E. Richards, Mol. Phys. 7 (1964) 515.

[16] T.M. Klapötke, G. McIntyre, A. Schulz, J. Chem. Soc. Dalton Trans. (1996) 3237.

[17] T.M. Klapötke, Chem. Ber. 130 (1997) 443.

[18] I.C. Tornieporth-Oetting, T.M. Klapötke, Angew. Chem. Int. Ed. Engl. 34 (1995) 511.

[19] ORTEP Plotting: C.K. Johnson, Technical Report ORNL-5138, Oak Ridge, 1976.

[20] Pluto Plotting: S. Motherwell, University Chemical Laboratory, Cambridge, 1978.

[21] I.C. Tornieporth-Oetting, T.M. Klapötke, Chemical properties and structures of binary and ternary Se–N and Te–N species: application of X-ray and ab initio methods, in: M. Hargittai, I. Hargittai (Eds.), Advances in Molecular Structure Research, vol. 3, JAI Press, Greenwich, Connecticut, 1997, pp. 287–311.

[22] T.M. Klapötke, A. Schulz, Quantenmechanische Methoden in der Hauptgruppenchemie Spektrum, Heidelberg, 1996, pp. 92–100.

[23] (a) E.J. Gabe, Y. Le Page, J.-P. Charland, F.L. Lee, P.S. White, J. Appl. Crystallogr. 22 (1989) 384. (b) Y. Le Page, J. Appl. Crystallogr. 21 (1988) 1983. (c) Y. Le Page, E.J. Gabe, J. Appl. Crystallogr. 12 (1979) 464.

[24] International Tables for X-ray Crystallography, vol. 6, Kynoch, Birmingham, 1974.

[25] (a) HyperChem 4.0, Molecular Visualization and Simulation Program Package, Hypercube, Waterloo, Ont., 1994. (b) HyperChem 5.0, Molecular Visualization and Simulation Program Package, Hypercube, Gainesville, FL, 1997.

[26] (a) A.D. Bacon, M.C. Zerner, Theor. Chim. Acta 53 (1979) 21–54. (b) W.P. Anderson, W.D. Edwards, M.C. Zerner, Inorg. Chem. 25 (1986) 2728–2732.

[27] J.B. Forseman, A. Frisch, Exploring Chemistry with Electronic Structure Methods, 2nd ed., Gaussian, Pittsburgh, PA, 1996.

[28] A. Schulz, I.C. Tornieporth-Oetting, T.M. Klapötke, Inorg. Chem. 34 (1995) 4343.

[29] K. Nakamoto, Infrared and Raman Spectra of Inorganic and Coordination Compounds, Wiley, New York, 1986.